

THE BEHAVIOUR OF COARSE-GRAIN HAZ STEEL WITH SMALL DEFECTS DURING CYCLIC LOADING

VEDENJE JEKLA GROBOZRNEGA TVP Z NAPAKAMI PRI CIKLIČNI OBREMENITVI

Vladimir Gliha, Tomaž Vuherer

University of Maribor, Faculty of Mechanical Engineering, Smetanova 17, 2000 Maribor, Slovenia
vladimir.gliha@uni-mb.si/ tomaz.vuherer@uni-mb.si

Prejem rokopisa – received: 2006-05-17; sprejem za objavo – accepted for publication: 2007-01-15

The effects of small, artificial surface defects on the fatigue strength of coarse-grain HAZ material found at the weld toe were studied. The size of the defects did not exceed the grain size, which is the most relevant microstructural unit of polycrystalline metals. The artificial defects were made by indenting the material with a Vickers pyramid and by drilling holes. The samples of coarse-grain HAZ material were prepared using a welding thermal-cycle simulator or a furnace. The experimentally determined bending fatigue strength versus the properly evaluated defects size was compared with the propagation of long cracks. Residual stresses appear when making small artificial defects. The crack initiation from the defects was analysed and the influence of residual stresses is discussed.

Key words: HAZ, weld toe, coarse grain, fatigue strength, artificial defect, residual stresses, non-propagating crack

Raziskan je bil vpliv majhnih umetnih napak na dinamično trdnost grobozrnatega dela TVP ob robu zvarov. Napake niso bile večje od kristalnih zrn, ki so najbolj pomembna enota polikristalnih materialov. Umetne napake smo ustvarili z odtiskovanjem Vikesove piramide in vrtanjem. Preizkušance z grobozrnatim jeklom TVP smo pripravili v simulatorju termičnega cikla in v peči.

Eksperimentalno določeno upogibno dinamično trdnost v odvisnosti od velikosti napake smo primerjali s propagacijo dolgih razpok. S pripravo umetnih napak nastanejo zaostale napetosti. V razpravi je govor o začetku razpoke iz napak in o vplivu zaostalih napetosti.

Ključne besede: TVP, rob zvara, groba zrna, dinamična trdnost, umetne napake, stabilna razpoka

1 INTRODUCTION

Defects decrease the fatigue strength of welds. In the past, S-N curves were the only available tool to predict the fatigue life of real quality welds until LEFM concepts started to be applied to welds with macroscopic crack-like defects.

Murakami and co-workers treated the influence of variously shaped small defects in the same way as cracks, i.e., using LEFM concepts¹⁻³. The square root of the projection of defects onto the plane perpendicular to the cyclic stress is a parameter reflecting the effect of small defects on the fatigue strength of metallic materials. However, LEFM greatly underestimates the propagation rates of short cracks within the local plastic zones that develop as a result of the stress concentration^{4,5}.

Small cracks, much smaller than the smallest microstructural units (microstructurally small defects), have no influence on the fatigue strength of metals (endurance limit) although these cracks can propagate unexpectedly quickly at the beginning. Nevertheless, the propagation decelerates gradually when approaching microstructural obstacles such as grain boundaries. The propagation can even stop, and the cracks then become non-propagating. However, in the presence of cracks whose size is comparable to the microstructural units of a metal, the fatigue strength of metals is lowered. The behaviour of metals with cracks from the smallest (short

cracks) to the biggest (long cracks) is described with the use of a Kitagawa-Takahashi diagram⁶.

The crack-initiation times in the highest-quality butt-welds are shorter than predicted by LEFM if the cracks initiate at the weld toe. Therefore, the possibility of crack initiation at the weld toe, where a substantial stress concentration exists, is of greatest importance for the load-carrying capacity of cyclically loaded welded structures (**Figure 1**). Because of the concentrated stress,

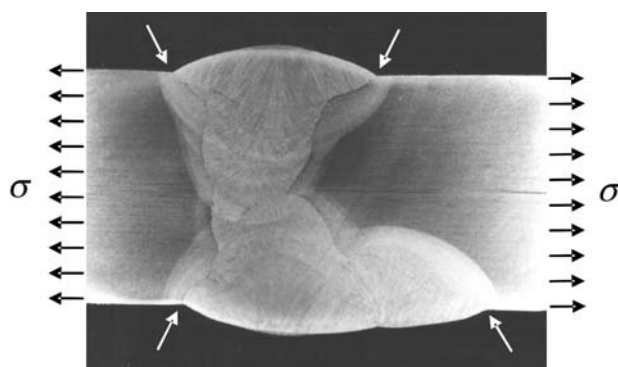


Figure 1: Macrograph of a K-butt weld with a remote homogeneous stress. Arrows indicate the weld toes: the positions of the concentrated stress field.

Slika 1: Makrografija K-zvara s homogeno napetostjo daleč od spoja. Puščice označujejo robove zvarov in položaj koncentriranega polja napetosti.

Table 1: Simulation parameters, mechanical properties, microstructures and test conditions**Tabela 1:** Parametri simulacije, mehanske lastnosti, mikrostrukture in pogoji preizkušanja

Designation	Cooling time t/s	Yield strength /MPa	Tensile strength /MPa	Grain size $d/\mu\text{m}$	Microstructure	Condition
M1	5	981	1210	130	M	C ₁ , C ₂ , C ₃ , C ₄ , C ₆
M2	9	935	1171	140	M+B	C ₁ , C ₂ , C ₄ , C ₆
M3	5.5	992	1192	180	M	C ₁ , C ₂ , C ₄ , C ₆
M4	9.5	939	1176	140	M+B	C ₁ , C ₂ , C ₄ , C ₅ , C ₆
M5	9.5	921	1172	180	M+B	C ₁ , C ₂ , C ₄ , C ₅ , C ₆

cracks at the weld toe initiate in the coarse-grain region of the HAZ, the formation of which is the result of the heat input needed for the fusion welding and, as a rule, it is much harder than the base metal ⁷.

Artificial defects, especially small holes, are used with great success in studies of the effects of small defects on the endurance limit of metallic materials. Extremely small weld defects, such as sharp transitions, inclusions, scratches or cracks, present at the weld toe, i.e., in the coarse-grain HAZ, can be modelled with artificial defects, too.

Vickers indentations are suitable artificial defects. The preparation of a proper indentation of the prescribed size is easy to execute because only the hardness has to be known. The problem of Vickers indentations used as artificial weld defects is residual stresses. Any kind of defect made in a mechanical way results in the appearance of residual stresses. The reason is in the irreversibility of the plastic deformation, which is very extensive when indenting with Vickers pyramids. High residual stresses affect the local stress/strain conditions and change the actual shape of the artificial defect.

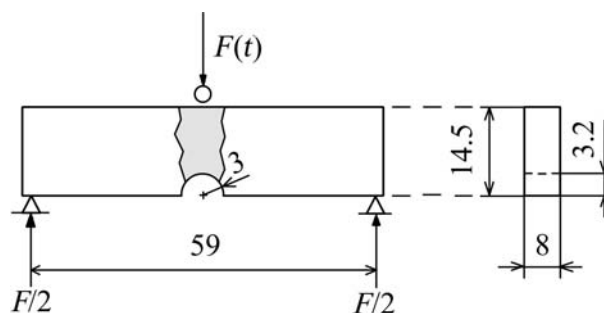
The behaviour of coarse-grain HAZ materials with different types of microstructurally small defects in a stress-concentrated condition was studied for cyclic loading. The effects of the residual stresses were taken into account.

2 EXPERIMENTAL

For this study samples of coarse-grained steel characteristic of the HAZ at the weld toe in the as-welded condition in the case of "cold" welding were prepared by simulating the thermal conditions in the material close to the weld on a welding thermal-cycle simulator (Smitweld). The coarse-grain microstructure was either pure martensite (M) or martensite with a small portion of bainite (M+B).

The simulated coarse-grain HAZ microstructures were designated as M1–M5. They were formed at different cooling rates. The data on the cooling times, the mechanical properties and the microstructures are shown in **Table 1**.

The specimens for the fatigue-strength testing were machined from samples with the simulated HAZ microstructure with the shape and size shown in **Figure 2**.

**Figure 2:** Bend specimen with a notch in the simulated coarse-grain HAZ steel**Slika 2:** Upogibni preizkušanci z zarezo na področju z jeklom simuliranega grobozrnatega TVP

The specimens were notched in the region with the simulated HAZ microstructure. The bottom of the notch was ground and polished. The calculated stress concentration caused by the notch was 1.74. The smooth surface at the bottom of the notch is specified in Table 1 as test condition C₁.

Artificial defects of different sizes and shapes were made by indenting with a Vickers pyramid on the bottom of the notch. As shown in Figure 3, they were single indentations and a series of five indentations in a straight line, perpendicular to the testing stress.

The average size of the single indentations, d , was (105, 160, and 221) μm . These situations are specified in Table 1 as the test conditions C₂, C₃ and C₄.

The average length of a series of indentations, l , was 386 μm and 692 μm . These situations are specified in Table 1 as the test conditions C₅ and C₆. The series were composed of indentations with diagonals of length of approximately 110 μm and 220 μm .

In the second part of this study, a coarse-grain HAZ was prepared with furnace heating. During the first step the samples of steel were heated to 1100 °C and held for 3 h. The grains grew to a size of 200 μm . This coarse-grain annealing was followed by cooling in water. The next step of the thermal treatment was heating to 870 °C and water quenching. The result of the combined thermal treatment was a microstructure of pure martensite.

The specimens were notched and artificial defects made either before or after the quenching.

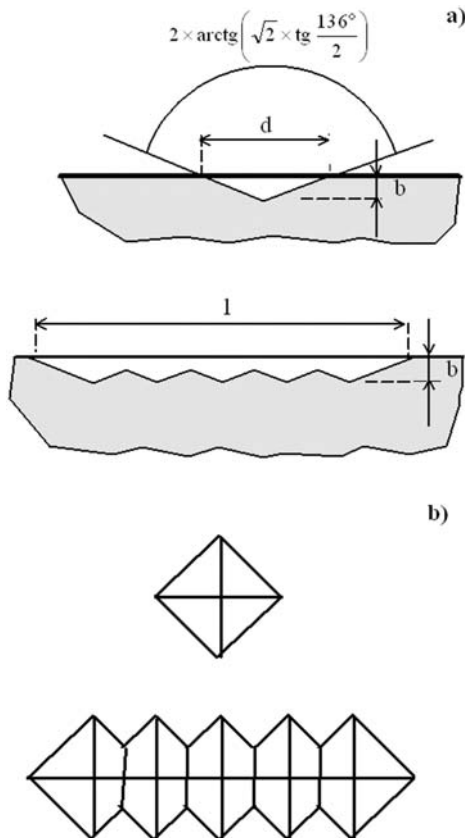


Figure 3: Small artificial surface defects: a single indentation with diagonal d and a series of five indentations with length l (cross-section – a, ground plan – b)

Slika 3: Majhne umetne površinske napake: odtis z diagonalo d in niz petih odtisov z dolžino l (prez – a, naris – b)

3 EXPERIMENTAL RESULTS AND DISCUSSION

Smooth and artificially surface-defected specimens were bend-loaded in the first part of this study on a resonant machine at room temperature in the load-control mode. The frequency of the loading and the stress rate were $f \cong 115$ Hz and $R \cong 0$, respectively.

The loading was increased in steps to 2 million cycles or to fatigue crack initiation or specimen fracture. A new specimen was used each time. The results of the testing were S-N curves, valid for the test condition C_1 – C_6 , and the coarse-grain HAZ materials M1–M5. The

highest stress range, $\Delta\sigma_B$, at which the material still resisted after 2 million cycles was taken as the bending fatigue strength of the material, $\Delta\sigma_{f-B}$. The numerical results of the testing are shown in **Table 2**.

The depth of the artificial defects, b in **Figure 3**, is an important parameter for the $\sqrt{\text{area}}$ evaluation, which depends on the size of the indentation. The angle between the opposite planes at the top of the Vickers pyramid is 136° . The angle, α , between the opposite edges that form the diagonal of the indentation, is therefore somewhat bigger:

$$\alpha = 2\text{arctg}\left(\sqrt{2} \cdot \text{tg} \frac{136^\circ}{2}\right); b = \frac{d\sqrt{2}}{4} \cdot \text{ctg} \frac{136^\circ}{2} \quad (1)$$

The defect size parameter $\sqrt{\text{area}}$ was evaluated for each of the used artificial defects, single indentations of three sizes and a series of indentations of two sizes. A special approach for the evaluation of long-shallow small defects is available ⁸.

As shown in **Figure 4**, the area is the plane of the actual defect projection for the single indentation and the product of the maximum defect width with the length of ten times the depth for the series of indentations ⁸.

$$\text{area}_{\text{ind}} = \frac{d^2\sqrt{2}}{8} \text{ctg} \frac{136^\circ}{2}; \text{area}_{\text{ind}} = \frac{5d^2\sqrt{2}}{4} \text{ctg}^2 \frac{136^\circ}{2} \quad (2)$$

The relationships between the results of the testing expressed as the fatigue strength $\Delta\sigma_{f-B}$ and the parameter $\sqrt{\text{area}}$ are shown on a logarithmic-logarithmic scale in **Figure 5**.

The shapes of the curves in **Figure 5** agree quite well with the Kitagawa-Takahashi plot. For that reason, three dotted lines are entered in the figure, representing the possible fatigue strengths of coarse-grained HAZ materials with long cracks. One of these lines could be the right-hand side of the Kitagawa-Takahashi plot because

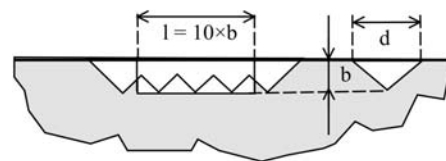


Figure 4: Size of the image of a series of indentations and a single indentation

Slika 4: Velikost ploščine niza odtisov in enega odtisa

Table 2: Fatigue strength of the HAZs in terms of the quality of the surface at the bottom of the notch

Tabela 2: Trajna dinamična trdnost TVP pri različni kakovosti površine na dnu zareze

Test condition	C_1	C_2	C_3	C_4	C_5	C_6
Defect size, μm	0	$d \cong 105$	$d \cong 160$	$d \cong 221$	$l \cong 386$	$l \cong 692$
Material	$\Delta\sigma_{f-B}/\text{MPa}$					
M1	539	526	520	481	–	442
M2	546	507	–	468	–	442
M3	533	520	–	468	–	416
M4	533	533	507	442	–	416
M5	526	520	–	468	481	416

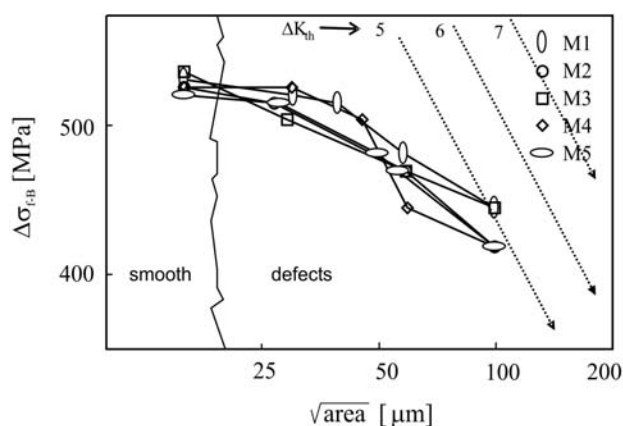


Figure 5: Dependence of the bending fatigue strength on the defect size parameter $\sqrt{\text{area}}$, calculated as illustrated in **Figure 4**

Slika 5: Odvisnost med upogibno dinamično trdnostjo in parametrom velikosti napake $\sqrt{\text{area}}$, izračunananim tako, kot je prikazano na **sliki 4**

the ΔK_{th} -value for carbon structural steels corresponds to 5–10 MPa $\sqrt{\text{m}}$.

Smooth and artificially surface-defected specimens were bend-loaded in the second part of this study on a rotary bending machine at room temperature in the load-control mode. The frequency of the loading and the stress rate were $f \cong 100$ Hz and $R = -1$, respectively. Single Vickers indentations and drilled small holes were used as artificial weld defects. The defect size parameter $\sqrt{\text{area}}$ was the same for both types of defect. Two examples of these defects with already-initiated cracks are shown in **Figures 6 and 7**.

The life of fatigue cracks has two stages: initiation and propagation. The crack initiation from defects in the presence of residual stresses is either easier or more difficult because of the locally enhanced or reduced stress/strain field caused by the defect preparation. Due to the existing pre-stress, the local stress rate, R , is changed. During the fatigue loading, at a sufficiently

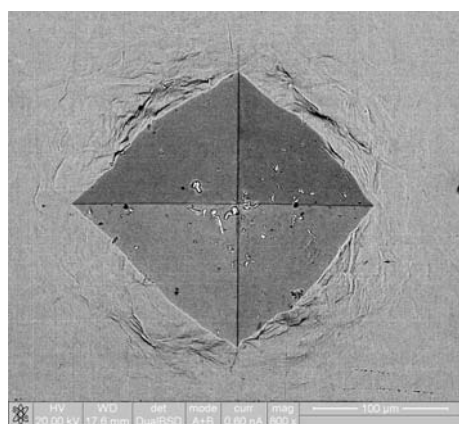


Figure 6: Vickers indentation with a diagonal of 200 μm . Cracks are visible at the ends of the indentation.

Slika 6: Vickers odtis z diagonalo 200 μm . Razpoki vidimo na konceh odtisa.

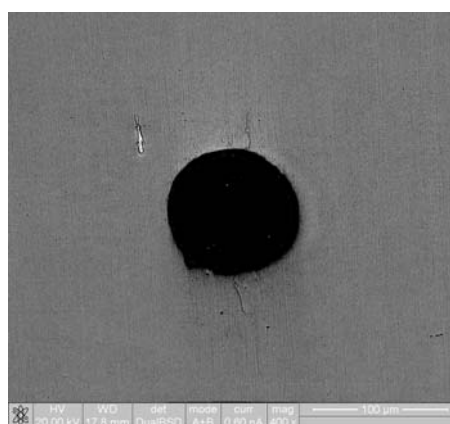


Figure 7: Drilled hole with a diameter of 90 μm . Cracks are initiated on both sides of the hole.

Slika 7: Izvrtina s premerom 90 μm . Razpoki nastaneta na obeh straneh izvrtine.

high stress level, cracks appear due to the interactive effect of the micro-defect and the loading.

To distinguish between the effects of micro-structurally small defects assisted by local residual stresses and microstructurally small defects acting alone, a suitable approach to remove those stresses was necessary. Electro-etching was not effective enough with indentations, although it is often used with drilled holes. Recrystallization in the last stage of CGHAZ simulation using a furnace seemed a convenient way to remove the local residual stresses without significantly changing the defect's geometry.

Two kinds of specimens with artificial defects were prepared:

- specimens in the as-indentated or as-drilled condition
- specimens in the stress-relieved condition

Local residual stresses due to indenting are compressive, whilst with drilling they could be tensile. When the defect is made before heating for water quenching, local residual stresses do not exist after quenching. The reason is the newly formed microstructure, caused by recrystallization during the transformation. In contrast, the introduction of the defect after the complete thermal treatment for coarse-grain HAZ simulation induces local residual stresses.

In the first stage of fatigue testing, a microcrack appears either at the surface, adjacent to the defects, or inside the defects. Crack initiation occurs in individual grains where the cyclic tangential stress in the weakest crystal plane of randomly oriented grains exceeds a determined level. If the remote stress level is not too high the grain boundary arrests the crack propagation. Local stress concentration due to the presence of defects assists the crack initiation, but the effect is reduced with the distance.

An array of initiated cracks on a specimen with a smooth surface is seen in **Figure 8**. The cracks are not longer than the average grain size, i.e., 200 μm . Their orientation in the initiation stage is close to $\pm \pi/4$.

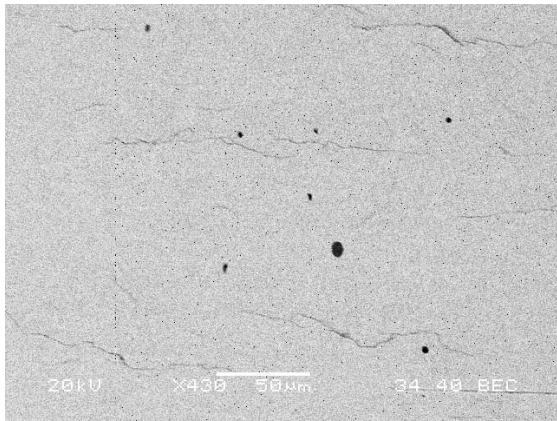


Figure 8: Cracks initiated at the bottom of the notched specimen without defects

Slika 8: Razpoke, ki so nastale na dnu zareze, ko ni napak

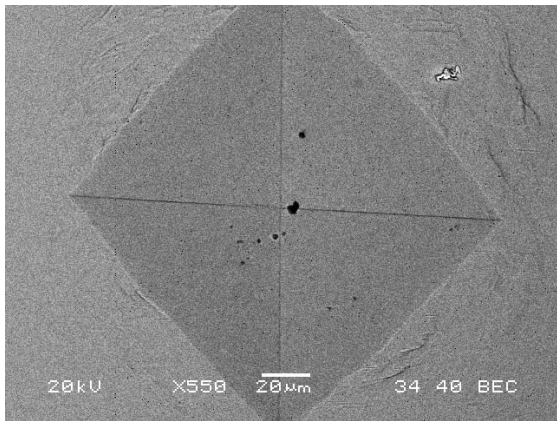


Figure 9: Two cracks initiated at both edges of a Vickers indentation

Slika 9: Razpoki, ki sta nastali na obeh robovih Vickers odtisa

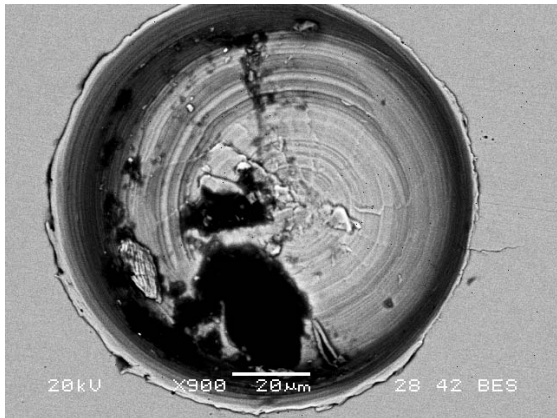


Figure 10: A single crack initiated from a hole

Slika 10: Ena sama razpoka, ki je nastala na izvrtini

In specimens where the crack is defected initiation turns up in part of the grains where the intensity of the cyclic stress/strain field is sufficient and it is parallel to the shearing direction of the grain.

Figure 9 represents two separate cracks initiated at the edges of the indentation. They are not connected at the bottom of the indentation and did not spread over the surface outside the indentation like the crack shown in **Figure 6**. The reason for this is the existence of compressive residual stresses, mostly at the bottom of the indentation.

Figure 10 shows a single crack initiated at the edge of a round hole. The difference between the two cracks in **Figure 7** and the single crack in **Figure 10** is explained by the absence of tensile residual stresses in the close vicinity of the hole. Only the grain with the initiated crack was oriented to enable crack initiation, the orientation of the grain on the other side was less suitable.

4 CONCLUSIONS

The shape of the relationship curve presenting the bending fatigue strength, $\Delta\sigma_{f,B}$, versus the defect size parameter $\sqrt{\text{area}}$ shown in Figure 5 does not approach the expected linear trend defined with several ΔK_{th} -values up to the defect size parameter $\sqrt{\text{area}} \cong 100 \mu\text{m}$. This is not surprising, because the threshold stress-intensity factor, ΔK_{th} , which defines the fatigue strength of materials with macroscopic cracks (the long-crack propagation law) is grain-size dependent. Because of coarse grains the ΔK_{th} -value is very likely much higher than 7. On the other hand, it seems that the defect size parameter $\sqrt{\text{area}}$ underestimates the fatigue strength, thereby lowering the effect of a series of indentations.

At this point it is not possible to conclude what is more important for the unexpected shape of the relationship curve $\Delta\sigma_{f,B}-\sqrt{\text{area}}$, the coarse grain size or the indenting residual stresses. The length of the biggest series of indentations is almost $700 \mu\text{m}$ (4–6 times the average grain size); the depth of the indentations does not exceed $31\text{--}32 \mu\text{m}$ (much less than the average grain size). A logical question is which extension of the series of indentations, length or depth, is more important? The answer – that it depends on which direction the cracks initiate – seems to be doubtful.

It was expected that specimens in the as-indenting condition would behave differently than those in the stress-relieved condition. The reason is the presence of the residual stresses:

If compressive residual stresses are the highest at the deepest part of the indentation, cracks will initiate separately at both loaded edges of the indentation. When the stress level is sufficiently low those cracks become non-propagating after their initiation. When stress level is higher the cracks join at the deepest part of the indentation and create a single crack. The effect of a bigger single crack is greater than the effect of separate cracks, although its size is almost equal to the sum of their lengths.

In the absence of residual stresses the crack will initiate as a single crack over the whole length of the indentation. An initiated crack in the stress-relieved condition that is longer than the indentation diagonal has a stronger effect than the effect of two separate cracks in the as-indented condition. The higher fatigue strength of the specimens with compressive residual stresses than those without residual stresses is logical.

Hole-drilled specimens behave differently than indented specimens. The residual stresses due to drilling are tensile; therefore, the opposite behaviour by the drilled specimens was observed. The fatigue strength of specimens with residual stresses is lower than the fatigue strength of specimens without residual stresses.

Generally, compressive stresses at the surface increase the fatigue strength, while the tensile stresses decrease it.

5 REFERENCES

- ¹ Murakami, Y. at al. Quantitative evaluation of effects of non-metallic inclusions on fatigue strength of high strength steels – I: Basic fatigue mechanism and evaluation of correlation between the fatigue fracture stress and the size and location of non-metallic inclusions, *Int. J. of Fatigue*, 9 (1989), 291–298
- ² Murakami, Y., Usuki, H. Quantitative evaluation of effects of non-metallic inclusions on fatigue strength of high strength steels – II: Fatigue limit evaluation based on statistics for extreme values of inclusion size, *Int. J. of Fatigue*, 9 (1989), 299–308
- ³ Murakami, Y. Effects of small defects and nonmetallic inclusions on fatigue strength of metals, *JSME International Journal I*, 32 (1989) 2, 167–180
- ⁴ Miller, K. J. The behaviour of short fatigue cracks and their initiation, Part I and Part II, *Fatigue Fract. Engng. Mater. Struct.*, 10 (1987) 1, 75–91 and 10 (1987) 2, 93–113
- ⁵ Yasniy P-V. at al. Microcrack initiation and growth in heat-resistant 15Kh2MFA steel under cyclic deformation, *Fatigue Fract. Engng. Mater. Struct.*, 28 (2005) 4, 391–397
- ⁶ Kitagawa, H., Takahashi, S. Applicability of fracture mechanics to very small cracks or the cracks in the early stage, 2nd International Conference on the Behaviour of Materials, Boston, ZDA, 1976
- ⁷ Verreman, Y., Bailon, J-P., Masounave, J. Fatigue life prediction of welded joints – A re-assessment, *Fatigue Fract. Engng. Mater. Struct.*, 10 (1987) 1, 17–36
- ⁸ Murakami, Y., Endo, M. Effects of hardness and crack geometries on ΔK_{th} of small cracks emanating from small defects, *The behaviour of short fatigue cracks*, Edited by K. J. Miller, E. R. de los Rios, Mechanical Engineering Publications, 1986